

62798



External Exposure To Radionuclides In Air, Water, And Soil

PB94-114451 Z

Federal Guidance Report No. 12

MAR 05 1999

REPRODUCED BY:
NATIONAL TECHNICAL INFORMATION SERVICE
U.S. DEPARTMENT OF COMMERCE
SPRINGFIELD, VIRGINIA 22161



11556

BIBLIOGRAPHIC INFORMATION

PB94-114461

Report Nos: none

Title: External Exposure to Radionuclides in Air, Water, and Soil. Exposure-to-Dose Coefficients for General Application, Based on the 1987 Federal Radiation Protection Guidance.

Date: 1993

Authors: K. F. Eckerman, and J. C. Ryman.

Performing Organization: Oak Ridge National Lab., TN.

Performing Organization Report Nos: EPA/402/R-93/081

Sponsoring Organization: *Environmental Protection Agency, Washington, DC. Office of Air and Radiation.

Type of Report and Period Covered: Federal guidance rept. no. 12.

Supplementary Notes: Sponsored by Environmental Protection Agency, Washington, DC. Office of Air and Radiation.

NTIS Field/Group Codes: 57B, 57K, 77B, 77E, 77F, 77G, 55E

Price: PC A11/MF A03

Availability: Available from the National Technical Information Service, Springfield, VA. 22161

Number of Pages: 240p

Keywords: *Radioactive isotopes, *Exposure, *Environmental monitoring, *Dosage, *Humans, Concentration(Composition), Tissues(Biology), Water pollution, Atmospheric chemistry, Land pollution, Tissues(Biology), Photons, Clouds(Meteorology), Soils, Path of pollutants, Estimates, Risk assessment, Safety, Bremsstrahlung, Skin cancer, Mathematical models, External, Radioactivity decay, Organs.

Abstract: The report tabulates dose coefficients for external exposure to photons and electrons emitted by radionuclides distributed in air, water, and soil. Dose coefficients for external exposure relate the doses to organs and tissues of the body to the concentrations of radionuclides in environmental media. Since the radiations arise outside the body, this is referred to as external exposure. This situation is in contrast to the intake of radionuclides by inhalation or ingestion, where the radiations are emitted inside the body. In either circumstance, the dosimetric quantities of interest are the radiation doses received by the more radiosensitive organs and tissues of the body. For external exposures, the kinds of radiation of concern are those sufficiently penetrating to traverse the overlying tissues of the body and deposit ionizing energy in radiosensitive organs and tissues. Penetrating radiations are limited to photons, including bremsstrahlung.

Continued on next page

BIBLIOGRAPHIC INFORMATION

Continued...

and electrons.

FB94-114451

SEP 20 1994

• 000000 •

PREFACE

Federal radiation protection guidance is developed by the Administrator of the Environmental Protection Agency as part of his or her responsibility, under Executive Order 10831, to "... advise the President with respect to radiation matters, directly or indirectly affecting health, including guidance for all Federal agencies in the formulation of radiation standards and in the establishment and execution of programs of cooperation with States." The purpose of Federal guidance is to provide a common framework to ensure that the regulation of exposure to ionizing radiation is carried out in a consistent and adequately protective manner.

This Federal guidance report is the third of a series designed to provide technical information useful in implementing radiation protection programs. It is our hope that it will help ensure that regulation of exposure to radiation is carried out in a consistent manner that makes use of the best available information for relating concentrations of radioisotopes in environmental media to dose in human populations due to external radiation. The dose coefficients in this report are intended for use by Federal agencies having regulatory responsibilities for protection of members of the public and/or workers, such as the Environmental Protection Agency, the Nuclear Regulatory Commission, and Occupational Health and Safety Administration, as well as by those Federal agencies with responsibilities related to the management of their own and their contractor operations, such as the Department of Energy and the Department of Defense. We also encourage their use by State and local authorities.

Exposure to external radiation from contaminated soil, which is a central focus of the calculations carried out to produce this report, is a particularly timely subject. The Nation is at the beginning of perhaps the largest cleanup operation in its history, at the large collection of sites involved in the development of nuclear weapons and commercial nuclear power during the past half century. An accurate assessment of this exposure pathway is essential to the decisions that will be required to regulate, manage, and verify this cleanup.

The principal dose quantity, effective dose equivalent, has been calculated with the weighting factors used in Federal Guidance Report No. 11, which were those recommended in Radiation Protection Guidance to Federal Agencies for Occupational Exposure (EPA, 1987).

New estimates of radiation risk to the organs and tissues have been published since then (UNSCEAR, 1988; NAS, 1990) and updated weighting factors have been recommended by the International Commission on Radiological Protection (ICRP, 1991). However, new weighting factors have not yet been adopted for use in the United States and would require a number of adjustments to existing regulations. As the report notes, for most radionuclides these dose coefficients are not very sensitive to the choice of weighting factors. We are reviewing new weighting factors, as well as EPA's own estimates of organ-specific risk factors, and we will propose changes in the weighting factors as soon as it appears necessary and reasonable to do so. At that time, we will also publish revised versions of this report and of Federal Guidance Report No. 11.

The tables in this report are also available as computer files so that they may be more easily used in programs for assessing dose. We are simultaneously making the tables for internal exposure contained in Federal Guidance Report No. 11 available in the same format. Instructions for obtaining both of these sets of computer files may be found at the back of this report.

We gratefully acknowledge the work of the authors, Keith F. Eckerman and Jeffrey C. Ryman, without whose outstanding contributions over the past several decades tables such as these would not exist. This project was made possible through joint funding from three Federal agencies: the Department of Energy (DOE), the Nuclear Regulatory Commission (NRC), and the Environmental Protection Agency. We appreciate the consistent support of the DOE and NRC project officers, C. Welty and N. Varma, and S. Yaniv and R. Meck, respectively, throughout the lengthy term of this work. We also are indebted to H. Beck, S. Y. Chen, C. M. Eisenhauer, P. Jacob, G. D. Kerr, D. C. Kocher, and C. B. Nelson for their technical reviews. The report has been clarified and strengthened through their efforts. We would appreciate being informed of any errors or suggestions for improvements so that these may be taken into account in future editions. Comments should be addressed to Allan C. B. Richardson, Deputy Director for Federal Guidance, Criteria and Standards Division (6602J), U. S. Environmental Protection Agency, Washington, DC 20460.


Margo T. Oge, Director
Office of Radiation and Indoor Air

PB94-114451

FEDERAL GUIDANCE REPORT NO. 12

EXTERNAL EXPOSURE TO RADIONUCLIDES IN AIR, WATER, AND SOIL

Exposure-to-Dose Coefficients for General Application,
Based on the 1987 Federal Radiation Protection Guidance

Keith F. Eckerman and Jeffrey C. Ryman

Oak Ridge National Laboratory
Oak Ridge, Tennessee 37831

Office of Radiation and Indoor Air
U.S. Environmental Protection Agency
Washington, DC 20460

1993

PROTECTED UNDER INTERNATIONAL COPYRIGHT
ALL RIGHTS RESERVED
NATIONAL TECHNICAL INFORMATION SERVICE
U.S. DEPARTMENT OF COMMERCE

CONFIDENTIAL

CONTENTS

I. INTRODUCTION	1
II. CALCULATIONAL METHODS	5
Dosimetric quantities	5
Organ doses from monoenergetic environmental photon sources	8
General description of the calculations	9
Description of the environmental sources	11
The radiation field from a semi-infinite cloud source	13
The radiation field from an infinite water source	14
The radiation field from contaminated soil sources	16
Organ dose from an isotropic field	18
Organ dose from contaminated soil	21
Discussion	35
Skin doses from monoenergetic environmental electron sources	48
Immersion in contaminated water	49
Submersion in contaminated air	50
Exposure to contaminated soil	52
Dose coefficient formulation for radionuclides	54
Relationship to Federal Guidance Report No. 11	55
III. TABLES OF DOSE COEFFICIENTS	57
IV. APPLICATION CONSIDERATIONS	183
Radionuclide decay chains	183
Spontaneous fission	184
Models of the human body	184
Pathway-specific modifying factors and exposures	185
Ground roughness	186
Non-uniform volume source distributions	187
Contaminated shorelines	187
Exposure during boating activities	188
Effects of indoor residence	189
Conclusions	192
APPENDIX A. NUCLEAR DECAY DATA	193
APPENDIX B. MODIFICATIONS TO THE HUMAN PHANTOM	213
APPENDIX C. EXTERNAL BREMSSTRAHLUNG	215

1. 000000. FGR

LIST OF FIGURES

II.1.	Calculation of radiation field due to a contaminated ground plane, on a cylinder surrounding the phantom location	12
II.2.	Calculation of organ dose from an angular current source on the cylinder surrounding the phantom	12
II.3.	Typical energy spectrum of scattered photons for submersion in a 1 Bq m^{-3} 100 keV contaminated air source.	15
II.4.	Typical energy spectrum of scattered photons for immersion in in a 1 Bq m^{-3} 100 keV contaminated water source.	15
II.5.	Angular dependence of air kerma for a 1 Bq m^{-3} 100 keV isotropic plane surface source	19
II.6.	Angular dependence of air kerma for a 1 Bq m^{-3} 100 keV isotropic plane source 0.2 mean free paths deep	19
II.7.	Angular dependence of air kerma for a 1 Bq m^{-3} 100 keV isotropic plane source 1 mean free path deep	20
II.8.	Angular dependence of air kerma for a 1 Bq m^{-3} 100 keV isotropic plane source 4 mean free paths deep	20
II.9.	Normalized effective dose equivalent for an isotropic plane surface source, submersion in a semi-infinite cloud, and immersion in an infinite water pool	36
II.10.	Comparison of normalized effective dose equivalent for an isotropic plane surface source and for water immersion to that for submersion	36
II.11.	Effective dose equivalent for submersion normalized to air kerma 1 m above the air-ground interface	37
II.12.	Comparison of normalized effective dose equivalent for submersion from this work (FGR 12) to that of Zankl et al.	37
II.13.	Effective dose equivalent normalized to air kerma 1 m above the air-ground interface for an infinite plane source 0.5 g cm^{-2} deep	38
II.14.	Comparison of normalized effective dose equivalent from this work to that of Zankl et al. for an infinite plane source 0.5 g cm^{-2} deep	38
II.15.	Effective dose equivalent normalized to air kerma 1 m above the air-ground interface for an infinite plane source at the interface	39
II.16.	Ratio of effective dose equivalent for rotational exposure to that for the actual field	39
II.17.	Effective dose equivalent, normalized to air kerma 1 m above the air-ground interface, for an infinite plane source at the interface, compared to Chen	41
II.18.	Ratio of normalized effective dose equivalent from Fig. II.15 to that of Chen from Fig. II.17 for an infinite plane source at the air-ground interface	41
II.19.	Effective dose equivalent normalized to air kerma for rotational normal beam exposure	42

II.20. Ratio of effective dose equivalent for rotational exposure from this report (FGR 12) to that from ICRP Publication 51	42
II.21. Effective dose equivalent normalized to air kerma 1 m above the air-ground interface, from an infinitely thick uniformly distributed soil source	45
II.22. Ratio of air kerma 1 m above 10 cm thick sources in soils of varying composition to that above the typical silty soil used in this report	47
II.23. Ratio of linear attenuation coefficient for the typical silty soil used in this report to that of other soils	48
II.24. Electron skin dose coefficient for immersion in contaminated water	50
II.25. Electron skin dose coefficient for submersion in contaminated air	51
II.26. Electron skin dose coefficients for exposure to contaminated soil	53
C.1. External bremsstrahlung spectrum of ^{85}Kr in air	220

CONFIDENTIAL

I. INTRODUCTION

This report tabulates dose coefficients for external exposure to photons and electrons emitted by radionuclides distributed in air, water, and soil. It is intended to be a companion to Federal Guidance Report No. 11 (Eckerman et al., 1988), which tabulated dose coefficients for the committed dose equivalent to tissues of the body per unit activity of inhaled or ingested radionuclides. The dose coefficients for exposure to external radiation presented here are intended for the use of Federal agencies in calculating the dose equivalent to organs and tissues of the body, as were those in Federal Guidance Report No. 11. Note that the dose coefficients for air submersion in this report update those given in Federal Guidance Report No. 11.

These dose coefficients are based on previously developed dosimetric methodologies, but include the results of new calculations of the energy and angular distributions of the radiations incident upon the body and the transport of these radiations within the body. Particular effort was devoted to expanding the information available for the assessment of the radiation dose from radionuclides distributed on or below the surface of the ground. Details of the underlying calculations and of changes from previous work are presented in Section II and in the appendices.

Dose coefficients for external exposure relate the doses to organs and tissues of the body to the concentrations of radionuclides in environmental media. Since the radiations arise outside the body, this is referred to as external exposure. This situation is in contrast to the intake of radionuclides by inhalation or ingestion, where the radiations are emitted inside the body. In either circumstance, the dosimetric quantities of interest are the radiation doses received by the more radiosensitive organs and tissues of the body. For external exposures, the kinds of radiation of concern are those sufficiently penetrating to traverse the overlying tissues of the body and deposit ionizing energy in radiosensitive organs and tissues. Penetrating radiations are limited to photons, including bremsstrahlung, and electrons. The radiation dose depends strongly on the temporal and spatial distribution of the radionuclide to which a human is exposed. The modes considered here for external exposure are:

- submersion in a contaminated atmospheric cloud, i.e., air submersion,
- immersion in contaminated water, i.e., water immersion, and
- exposure to contamination on or in the ground, i.e., ground exposure.

Estimation of the dose to tissues of the body from radiations emitted by an arbitrary distribution of a radionuclide in an environmental medium is an extremely difficult computational task. Therefore, it has become common practice to consider simplified and idealized exposure geometries; i.e., the radionuclide concentration in the medium, seen from the location of an exposed individual, is uniform and effectively infinite or semi-infinite in extent. In particular, a semi-infinite source region is assumed for submersion in contaminated air (Poston and Snyder, 1974) and an infinite source region is assumed for immersion in contaminated water and exposures to contaminated soil (Kocher, 1981). Even for simplified geometries, calculation of the energy and angular distributions of radiations incident on the body and the transport of radiation within the body is a demanding computational problem.

If one assumes an infinite or semi-infinite source region with a uniform concentration $C(t)$ of a radionuclide at time t , then the dose equivalent in tissue T , H_T , can be expressed as

$$H_T = h_T \int C(t) dt \quad (1)$$

where h_T denotes the time-independent dose coefficient for external exposure. The coefficient h_T represents the dose to tissue T of the body per unit time-integrated exposure, expressed in terms of the time-integrated concentration of the radionuclide; that is, h_T is defined as

$$h_T = \frac{H_T}{\int C(t) dt} \quad (2)$$

An alternative interpretation considers h_T to represent the instantaneous dose rate in organ T per unit activity concentration of the radionuclide in the environment. In most applications, the dose H_T , not the instantaneous dose rate, is the quantity of interest, and thus the time integral of the concentration must be evaluated. Note that limits of integration have not been specified in Eqs. (1) and (2) since they depend upon the nature of the dose quantity H_T . For example, if H_T is to represent the dose associated with a single year of exposure then the integration in Eq. (1) would range from t_0 to $t_0 + 1$ years, where t_0 is the year of interest. However, if it were to represent the dose associated with a particular practice, e.g., annual emissions from a facility, then the integral might range over many years as the emitted radionuclide persists in the environment. Depending on the nature of the application it may be advantageous to view the numerical value of the coefficient h_T as either the instantaneous dose rate per unit concentration or as the dose per unit time-integrated concentration. In this report we follow the latter presentation.

The dose coefficient h_r for a specific radionuclide is uniquely determined by the type, intensity, and energy of the emitted radiations, the mode of exposure, and the anatomical variables that govern the energy deposition in organ or tissue T . The dose coefficient incorporates the transport of emitted radiations in the environment, their subsequent transport in the body, and estimation of the deposition of ionizing energy in the tissues of the body. Calculations of dose coefficients, as performed for this report, involve three major steps:

- (1) computation of the energy and angular distributions of the radiations incident on the body for a range of initial energies of monoenergetic sources distributed in environmental media of interest;
- (2) evaluation of the transport and energy deposition in organs and tissues of the body of the incident radiations, characterized above in terms of their energy and angular distributions, for each of the initial energies considered; and
- (3) calculation of the organ or tissue dose for specific radionuclides, considering the energies and intensities of the radiations emitted during nuclear transformations of those nuclides.

The result of the first two steps is a set of dose coefficients for monoenergetic sources of photon or electron radiations. The last step simply scales these coefficients to the emissions of the radionuclides of interest.

A number of reports have tabulated dose coefficients for external irradiation of the body from radionuclides distributed in the environment (Poston and Snyder, 1974; Dillman, 1974; O'Brien and Sanna, 1978; Koblinger and Nagy, 1985; Jacob et al., 1986, 1988a, 1988b; Kocher, 1981, 1983; DOE, 1988; Saito et al., 1990; Chen, 1991; Petoussi et al., 1991). Because of limitations in computational methods or available information, some of these efforts have used oversimplified assumptions regarding the exposure conditions. For example, the radiations incident upon the body have often been assumed to be uniformly distributed in angle (an isotropic field) or to be incident perpendicular to the body surface while the body is uniformly rotated about its vertical axis (a rotational exposure). Variations in the intensity of the radiations with height above the ground frequently have been ignored in assessing the dose from radionuclides on or below the ground surface. In addition, bremsstrahlung has generally been ignored, despite the fact that for many radionuclides (e.g., pure beta emitters), it is the only source of radiation sufficiently penetrating in nature to result in a dose to underlying tissues of the body. In this report, we have attempted to address each of these aspects of the problem without the use of simplifying assumptions that would significantly alter the results.

quantities are weighted sums of the doses to radiosensitive tissues of the body. The effective dose equivalent H_D and the effective dose E , are defined as:

$$H_D = \sum_T w_T H_T \quad (3a)$$

and

$$E = \sum_T w'_T H_T \quad (3b)$$

where H_T is the mean dose equivalent to organ or tissue T, the w_T are a specific set of weighting factors, and the w'_T are a set of weighting factors not specified as part of the definition of E , and can take any assigned values. Thus, the effective dose equivalent can be interpreted as a particular example of the effective dose. Values for w_T and the current recommendations of the ICRP for w'_T are shown in Table II.1. The factors w_T and w'_T correspond to the fractional contribution of organ or tissue T to the total risk of stochastic health effects when the entire body is uniformly irradiated. As seen in Table II.1, the weighting factors currently recommended by the ICRP to compute the effective dose explicitly consider a greater number of organs and tissues of the body. In addition the two sets of weighting factors differ in the manner that the dose to tissues not explicitly identified (the remainder) is evaluated. Of a more fundamental nature, it should be noted that the measures of health detriment used to derive the two sets of weighting factors are different. The weighting factors for the effective dose equivalent characterize the health detriment in terms of the risk of fatal cancers and hereditary defects in the first two generations. In the case of the currently recommended factors for effective dose, the health detriment is characterized by a weighting of the risks for both fatal and nonfatal cancers, the risk of hereditary defects over all future generations, and the relative loss of life expectancy, given a fatal cancer or a severe genetic disorder.

Since no decision has been made, at the time of this report, on changes in weighting factors for use in the United States, the tabulations by radionuclide of the dose coefficients in this report are based on the weighting factors specified for the effective dose equivalent quantity, the quantity used in Federal Guidance Report No. 11 (Eckerman et al., 1988). However, the effective dose, computed with the weighting factors currently recommended by the ICRP, is included in many of the preliminary tabulations and discussions. The results indicate that for many radionuclides of practical significance, for the exposure geometries considered here, the differences are small - on the order of a few percent. However, in some cases the differences can be large, so that specification of the w_T is an important consideration. Zankl et al. (1992) have also investigated these differences for various external irradiation

geometries and a few key radionuclides and reach similar conclusions.

The coefficient relating the dose equivalent H_T in organ or tissue T to the time integral of the nuclide's concentration in the environment is denoted by h_T . The notation and tabulation of the dose coefficients presented in this report follow the conventions and format of Federal Guidance Report No. 11. The radionuclide tabulations include the coefficients for the gonads, breast, lung, red marrow, bone surface, thyroid, and remainder, followed by that for the effective dose equivalent. The coefficient for the remainder group is the average of the doses to each of the five tissues comprising the remainder and thus $w_T = 0.3$ is applied to this numerical value to compute the effective dose equivalent. Although skin is excluded from the effective dose equivalent, we have included it in the tabulations since it frequently is the most highly irradiated tissue for external exposure.

Table II.1. Tissue Weighting Factors According to ICRP (1977, 1991).

Organ/Tissue	Weighting Factors	
	w_T (ICRP 26)	w'_T (ICRP 60)
Gonads	0.25	0.20
Breast	0.15	0.05
Colon		0.12
Red Marrow	0.12	0.12
Lungs	0.12	0.12
Stomach		0.12
Urinary Bladder		0.05
Liver		0.05
Esophagus		0.05
Thyroid	0.03	0.05
Bone Surface	0.03	0.01
Skin		0.01
Remainder	0.30 ¹	0.05 ^{2,3}

¹ The value 0.30 is applied to the average dose among the five remaining organs or tissues receiving the highest dose, excluding the skin, lens of the eye, and the extremities.

² The remainder is composed of the following tissues and organs: adrenals, brain, small intestine, upper large intestine, kidney, muscle, pancreas, spleen, thymus, and uterus.

³ The value 0.05 is applied to the average dose to the remainder tissue group. However, if a member of the remainder receives a dose in excess of the highest dose in any of the twelve organs for which weighting factors are specified, a weighting factor of 0.025 is applied to that organ and a weighting factor of 0.025 is applied to the average dose in the rest of the remainder.

OH-000000-0000

Organ doses from monoenergetic environmental photon sources

The calculation of organ doses from irradiation of the human body by photon emitters distributed in the environment requires the solution of a complex radiation transport problem. It is impractical to solve this problem for the precise spectrum of photons emitted by each radionuclide of interest. Therefore, organ doses were computed for monoenergetic photon sources at twelve energies from 0.01 to 5.0 MeV. The results of these calculations were then used to derive the dose coefficients in Tables III.1 through III.7, taking into account the detailed photon spectrum of each radionuclide. The following pages describe the methods used to compute organ dose coefficients for those monoenergetic sources.

Previous estimates of submersion dose (Poston and Snyder, 1974; O'Brien and Sanna, 1978; Eckerman et al., 1980; Kocher, 1981, 1983; DOE, 1988) were based on Monte Carlo calculations with (1) poor statistics for some organ doses (due to the limitations of early computer systems) or (2) minor errors in sampling the radiation field. It should be noted that Saito et al. (1990) have recently published a compilation of organ doses due to air submersion based on modern Monte Carlo methods that appears to overcome these limitations.

The seminal work of Beck and de Planque (1968) on dose due to contaminated soil, while accurately reflecting the radiation field, was limited to calculation of air dose for energies between 0.25 and 2.25 MeV, although the data were later used to generate a tabulation of air exposure rates for a number of nuclides (Beck, 1980). The next generation of calculations (Kocher, 1981, 1983; DOE, 1988; Kocher and Sjoeren, 1985) produced useful dose estimates for many nuclides, but was limited by simplifying assumptions regarding the energy and angular dependence of the radiation field (assumed to be equivalent to that for submersion) and the use of the point kernel method for characterizing the field strength. More recent efforts (Williams et al., 1985; Kobliger and Nagy, 1985; Jacob et al., 1986, 1988a, 1988b; Saito et al., 1990; Petoussi et al., 1991) have used relatively sophisticated methods for analyzing the energy, angular, and spatial dependence of the radiation field and computing organ doses for both mathematical and CT-derived phantoms of various ages. These data are primarily for plane sources at or near the air-ground interface, or for naturally-occurring radionuclides distributed to effectively infinite depth in the soil. The calculations of Chen (1991) include volume sources of many thicknesses as well as plane sources at the interface, but are only for effective dose equivalent based upon rotational normal beam exposure (ICRP, 1987).

The computational methods used in this work were chosen to give an accurate characterization of the energy and angular dependence of the radiation field incident on the body, since dose to the body is very sensitive to the direction of incident radiation, and also to

overcome other limitations of earlier calculations. Organ doses were computed for 25 organs in an adult hermaphrodite phantom (Cristy and Eckerman, 1987). The mathematical phantom was modified, as described in Appendix B, to include the esophagus, a tissue given an explicit weighting factor in the current effective dose formulation of the ICRP (1991), and to improve the modeling of the neck and thyroid.

General description of the calculations

Estimating organ dose in a human phantom exposed to radiation from an external source consists of calculating an effect of interest in a geometrically complex object located in an otherwise geometrically simple (one- or two-dimensional) system. This process is mathematically described by the time-independent neutral-particle Boltzmann transport equation:

$$\bar{\nabla} \cdot \bar{\Omega} \Phi(\bar{r}, E, \bar{\Omega}) + \mu(\bar{r}, E) \Phi(\bar{r}, E, \bar{\Omega}) = \int dE' \int d\bar{\Omega}' \mu_s(\bar{r}, E' - E, \bar{\Omega}' - \bar{\Omega}) \Phi(\bar{r}, E', \bar{\Omega}') + S(\bar{r}, E, \bar{\Omega}) \quad (4)$$

where

- $\Phi(\bar{r}, E, \bar{\Omega}) dE d\bar{\Omega}$ = angular fluence at position \bar{r} with energy in dE about E and direction in solid angle $d\bar{\Omega}$ about direction $\bar{\Omega}$;
- $\mu(\bar{r}, E)$ = linear attenuation coefficient at position \bar{r} , and energy E ;
- $\mu_s(\bar{r}, E' - E, \bar{\Omega}' - \bar{\Omega}) dE d\bar{\Omega}$ = the probability per unit path length that a particle with initial energy E' and direction $\bar{\Omega}'$ will undergo a scattering collision at point \bar{r} and emerge with energy in dE about E and in $d\bar{\Omega}$ about $\bar{\Omega}$; and
- $S(\bar{r}, E, \bar{\Omega}) dE d\bar{\Omega}$ = number of source particles emitted at position \bar{r} with energy in dE about E and direction in $d\bar{\Omega}$ about $\bar{\Omega}$.

Equation (4) is conveniently written in operator notation as

$$\hat{H} \Phi(\bar{p}) = S(\bar{p}) \quad (5)$$

where \bar{p} represents position, energy, and direction phase space.

After the solution to Eq. (4) is obtained, the organ dose is computed from the following integral:

$$H_T = \int_{\bar{p}_T} \Phi(\bar{p}) R(\bar{p}) d\bar{p} \quad (6)$$

where

- H_T = the effect of interest, i.e., the organ dose;
- \bar{p}_T = phase space of tissue or organ T; and
- $R(\bar{p})$ = the response function, i.e., the contribution to H_T due to unit angular fluence.

In principle, Eqs. (5) and (6) can be solved directly using Monte Carlo methods. However, this direct approach involves a combination of deep penetration (i.e., transport through many mean free paths of air and/or soil) and complex geometry (the human phantom). Calculations of this type require the use of sophisticated variance reduction techniques to overcome the inherent statistical nature of the Monte Carlo method. Often, the important regions of phase space are undersampled, and the effect of interest is underestimated (Armstrong and Stevens, 1969). To avoid the difficulties associated with a direct Monte Carlo solution, the solution is broken into two steps, using an important property of the transport equation.

In a problem involving distributed radiation sources and an effect on a target (the organ dose), a model using a closed surface surrounding the target can be postulated to estimate the effect (a closed surface surrounding the sources is equivalent). One can also consider a second model in which the target and its surrounding medium are the same, but on the other side of the closed surface is a vacuum or a perfect absorber. In the second model, an area source is constructed on the closed surface such that the strength per unit area in each direction and at each energy, $S_{\lambda}(\vec{r}, \vec{\Omega}, E)$, at each point \vec{r} , on the surface is equal to the flow rate $J_{\lambda}(\vec{r}, \vec{\Omega}, E)$ at the corresponding point in the first problem. It is possible to show rigorously (Chilton et al., 1984) that the effect on the target (organ dose in this application) is the same for both problems. Therefore, the sources for the first model may be replaced by the flow rate they create at the closed surface bounding the second model.

The problem of computing organ dose from environmental photon sources may thus be broken into two independent steps: (1) the calculation of the radiation field incident on a closed surface surrounding the human phantom model, and (2) the calculation of organ dose due to a surface source equivalent to the angular flow rate entering the boundary surrounding the phantom. To eliminate the geometric complexity of the human phantom from the calculation of the incident radiation field, the phantom must be removed from the problem. This may be done if the presence of the phantom in the original problem does not significantly perturb the incoming angular flow rate across the boundary surrounding the phantom. The phantom can affect the incoming directions of the radiation field only for those photons which, having interacted in the phantom, pass out of the surrounding surface, scatter in the surrounding media, and return across the boundary. This should be, at most, a second-order effect. Saito et al. (1990) have demonstrated that this perturbation is, as expected, not significant.

For the environmental photon sources considered in this report, the calculation of organ dose was broken into two independent calculations, as described above. The calculation of the

radiation field due to a unit source strength was performed by methods appropriate to the kind of source, as described later. Then, an equivalent source was constructed on a cylindrical surface surrounding the phantom, and the organ doses resulting from this source were computed for all cases by the Monte Carlo method, also described later. The two steps of the calculation are illustrated in Figs. II.1 and II.2 for the case of a contaminated soil source (an isotropic plane source at depth d_s).

Description of the environmental sources

The source for the submersion dose calculations is a semi-infinite cloud containing a uniformly-distributed monoenergetic photon emitter of unit strength (1 Bq m^{-3}) surrounding a human phantom standing on the soil at the air-ground interface. The air composition, given in Table II.2, is for conditions of 40% relative humidity, a pressure of 760 mm Hg, a temperature of 20°C , and a density of 1.2 kg m^{-3} . The dose coefficients for submersion can be readily scaled to account for a different air density.

Table II.2. Air Composition

Element	Mass Fraction
H	0.00064
C	0.00014
N	0.75086
O	0.23555
Ar	0.01281
Total	1.00000

The source for the contaminated soil calculations is an infinite isotropic plane source of monoenergetic photons of unit strength (1 Bq m^{-2}), located at the air-ground interface or at a specified depth in the soil. Again, a human phantom is standing on the soil at the air-ground interface. As noted later, the organ dose due to a source in the soil that is uniformly distributed from the surface to a specified depth may be readily computed from the doses due to a series of plane sources at different depths. The air composition is the same as for the submersion dose calculations (see Table II.2). The assumed soil composition is given in Table II.3, and is that for a typical silty soil (Jacob et al., 1986) containing 30% water and 20% air by volume. The soil density was taken to be $1.6 \times 10^3 \text{ kg m}^{-3}$. It should be noted that the radiation field above the air-ground interface can, in some circumstances, be scaled to account for differences in soil

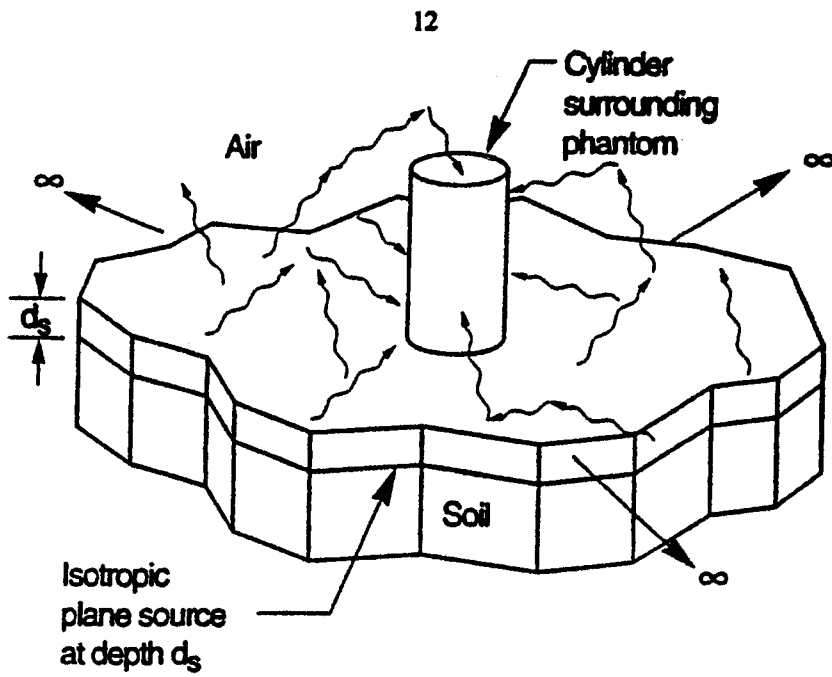


Fig. II.1. Calculation of radiation field due to a contaminated ground plane, on a cylinder surrounding the phantom location.

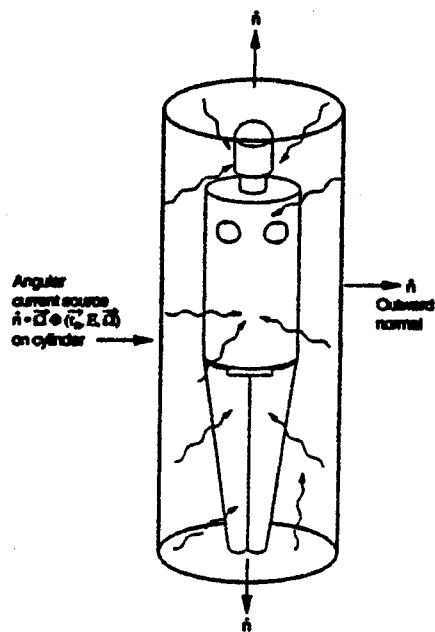


Fig. II.2. Calculation of organ dose from an angular current source on the cylinder surrounding the phantom.

density (Beck and de Planque, 1968; Chen, 1991). While the radiation field above the air-ground interface is relatively insensitive to soil composition for a plane surface source (Beck and de Planque, 1968), this is not true for distributed sources within the soil, as we later show.

Table II.3. Soil Composition

Element	Mass Fraction
H	0.021
C	0.016
O	0.577
Al	0.050
Si	0.271
K	0.013
Ca	0.041
Fe	0.011
Total	1.000

The source for the water immersion calculations is an infinite pool of water containing a uniformly-distributed monoenergetic photon emitter of unit strength (1 Bq m^{-3}). A human phantom is assumed to be completely immersed in the pool. The water density is $1.0 \times 10^3 \text{ kg m}^{-3}$ and the composition by mass fraction is 0.112 for H and 0.888 for O; i.e., pure water.

The radiation field from a semi-infinite cloud source

The dose near the air-ground interface from a semi-infinite cloud source has been taken to be one-half that due to an infinite cloud source, following the practice of Dillman (1974), Poston and Snyder (1974), and Kocher (1981, 1983). This has been shown (Ryman et al., 1981) to be a good approximation for air dose (within 20%) at energies of 20 keV or greater. At energies below 10 keV (the lowest energy considered here), the dose at the interface should still be one-half that due to an infinite source, but there will be an increase in dose with increasing height along the phantom. The mean free path of these photons is so short that the upper portions of the phantom are effectively exposed to an infinite source. Between 10 and 20 keV, there will be some increase in dose with increasing height, but since the increase over the dimensions of the body should be fairly small, it has not been considered here.

Given this approximation, the radiation field may be computed as that due to an infinite cloud source of a monoenergetic photon emitter. In this case, the transport equation (4) loses its dependence on spatial position and angle, and may be written, for scattered photons, as (Dillman, 1970, 1974)

$$f(E') = \mu(E') \phi'(E') = K(E', E_0) + \int_{E'}^{E_0} f(E) K(E', E) dE, \quad (7)$$

where

$\mu(E')$ = the linear attenuation coefficient of air at energy E' ;
 $f(E') dE'$ = the number of photons per initial photon with energy in dE' about E' ; and
 $K(E', E_0)$ = the probability per unit energy that a photon of initial energy E_0 will scatter and give rise to a photon of energy E' .

The scattered photon fluence is just

$$\phi^s(E) = \frac{S_v \times f(E)}{\mu(E)}, \quad (8)$$

where S_v is the source strength per unit volume. The uncollided fluence is easily shown to be

$$\phi^u(E_0) = \frac{S_v}{\mu(E_0)}. \quad (9)$$

An updated version of the PHOFLUX computer program, developed by Dillman (1974) to solve this Volterra-type integral equation, was used to compute the energy spectrum of scattered photons in an infinite cloud source as well as the intensity of uncollided photons. Photoelectric and pair production cross section data were taken from ENDF/B-V (Roussin et al., 1983). Klein-Nishina scattering cross sections were computed analytically. The resulting energy spectrum from a 100 keV source is shown in Fig. II.3. The discontinuity seen in the figure occurs at the minimum possible energy to which an initial photon may scatter. The slight bump corresponds to the minimum possible energy for a twice-scattered initial photon.

The radiation field from an infinite water source

In this case, no approximation to the source is necessary, and Eq. (7) above is directly applicable. The PHOFLUX program with ENDF/B-V cross sections was also used here to compute the energy spectrum of photons in an infinite water source. The resulting energy spectrum from a 100 keV source is presented in Fig. II.4.

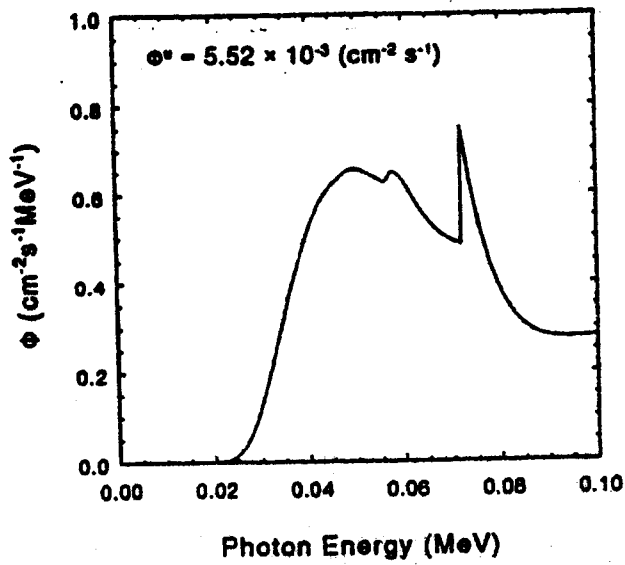


Fig. II.3. Energy spectrum of scattered photons for submersion in a 1 Bq m^{-3} 100 keV contaminated air source. ϕ^0 is the uncollided flux density.

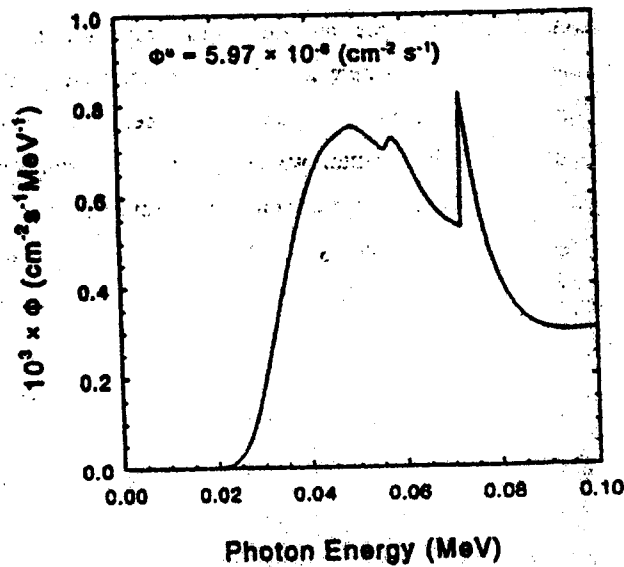


Fig. II.4. Energy spectrum of scattered photons for immersion in a 1 Bq m^{-3} 100 keV contaminated water source. ϕ^0 is the uncollided flux density.

41-00000-1

The radiation field from contaminated soil sources

In this case, the solution to the transport equation (4) is a function of only one spatial and one angular variable. It can be seen from Eq. (4) that the transport equation is linear with respect to the source term $S(\vec{r}, E, \vec{\Omega})$. Therefore, the fluence $\Phi(\vec{r}, E, \vec{\Omega})$ due to an isotropic infinite source uniformly distributed over a finite depth in the soil may be determined by superposition of the fluence for a series of isotropic infinite plane sources in soil.

The radiation field due to isotropic infinite plane sources at twelve energies from 0.01 to 5.0 MeV was computed for source depths of 0, 0.04, 0.2, 1.0, 2.5, and 4.0 mean free paths in soil (specified at the source energy). These depths were chosen to facilitate an accurate integration during the determination of the dose coefficients for sources uniformly distributed over specified depths. The uncollided angular photon fluence was computed analytically. A spatial-, energy-, and angular-dependent first collision source was generated from the uncollided angular fluence and the cross sections for scattering from the source energy into a series of energy groups. The scattered photon fluence due to the first-collision source was computed using the one-dimensional multigroup discrete ordinates method (Bell and Glasstone, 1970). Seventy energy groups between 5.3 and 0.00865 MeV were used. The group boundaries were selected to satisfy two criteria: (1) a relatively narrow group was present about each source energy of interest, and (2) photons scattering from any group could scatter to at least two other groups. A subset of the 70 groups was used for each source energy. The highest energy group was just that group containing the source, and the lowest group was that containing the low-energy cutoff, determined by $\lambda_s + 14$, where λ_s is the Compton wavelength (electron rest mass energy divided by photon energy) at the source energy. Since, by conservation of energy and momentum, the maximum change in Compton wavelength is 2 for a single scatter, a low-energy cutoff corresponding to $\lambda_s + 14$ ensures that a minimum of seven scatters is considered. Beck and de Planque (1968) state that a low-energy cutoff of $\lambda_s + 13.2$ included over 99% of the energy deposited in their air-dose calculations, except for the combination of very high source energies and very large interface-to-detector distances, which is not of interest here. The only exception to our use of the low-energy cutoff was for the 10 keV sources, in which case only 6 groups were used. At this energy, most photons are immediately absorbed, due to the high photoelectric cross section, and the scattered photon fluence decreases quite rapidly with decreasing energy.

In all calculations, the thickness of the air medium was three mean free paths (at the source energy). Photons scattered in the atmosphere at a height greater than three mean free paths must have traveled a minimum of six mean free paths from the source plane to reach the phantom location, and therefore cannot make a significant contribution to organ dose. For the

plane sources at depths of 0, 0.04, 0.2, and 1.0 mean free paths, the thickness of the soil medium was taken as three mean free paths (at the source energy). For the sources at depths of 2.5 and 4 mean free paths, the soil thicknesses were taken as 3.5 and 5 mean free paths, respectively. As in the case of air, photons scattered at depths beyond the lower soil boundary would have to travel a minimum of six mean free paths from the source plane to reach the phantom location, and thus make no significant contribution to organ dose.

In transport problems involving an isotropic plane source, the angular fluence has a singularity at the source plane for directions parallel to the plane (Fano et al., 1959) which cannot be accommodated by the discrete ordinates formulation used here, and which can also cause problems when the Monte Carlo method is used. To avoid the numerical problems associated with the singularity, the uncollided angular fluence is computed analytically. Then, a first-collision source; i.e., a distributed source based on the spatial, energy, and angular distribution of photons produced by the first collision of source photons, is calculated from the analytic uncollided angular fluence. In photon transport, a collision which leads to secondary photons can include pair production as well as Compton scatter. The first-collision source, averaged over the spatial mesh cells of the discrete ordinates formulation, is taken to be the source term in the transport equation, which is solved for the angular fluence of scattered photons. Cell-averaged angular first-collision sources have no singularities, even in cells adjacent to the source plane. It should also be noted that the scattered angular fluence has a singular component at the source plane, and, at short distances from the source, will have components of large magnitude in directions nearly parallel to the plane. It has been demonstrated (Ryman, 1979) that discrete ordinates calculations for the scattered fluence due to a first-collision source must use an angular mesh which has several directions nearly parallel to the source plane. Failure to do so will give rise to scalar fluences that are depressed or enhanced in a physically unrealistic manner in regions near the source. It is also well known (Bell and Glasstone, 1970) that for plane geometries, the fluence near an interface is better represented when the angular quadrature directions are chosen from a double- P_N Gauss quadrature set. Therefore, a DP_{13} quadrature set with 32 directions was selected for these calculations.

A discrete ordinates solution of the transport equation in which the cross sections are represented by truncated Legendre polynomial expansions can give rise to physically unrealistic negative angular fluences, due to the negative oscillations in the cross section expansions. This problem is worse for highly anisotropic sources, narrow energy groups, and highly anisotropic scatter, e.g., Compton scatter of photons. Several studies have demonstrated (Odom and Shultis, 1976; Mikols and Shultis, 1977; Ryman, 1979) that this problem may be eliminated by the use

of the exact-kernel cross section representation, i.e., use of a discrete scattering matrix rather than a polynomial representation. In this work, a one-dimensional multigroup discrete ordinates code (KSLAB1), developed by one of the authors (Ryman, 1979), which uses the exact-kernel representation of group-to-group transfer cross sections, was used to perform the radiation field calculations. The group-to-group transfer cross sections, which included Compton (Klein-Nishina) scattering and the production of annihilation radiation, when appropriate, were generated from the data of Biggs and Lighthill (1968, 1971, 1972a, 1972b). The spatial mesh in the air and the soil was tailored to each problem to ensure that (1) negative angular fluences were not generated as a result of a too-coarse mesh spacing, and (2) the angular fluence had converged with respect to mesh size.

The accuracy of the solutions was checked by comparing the energy and angular dependence of the air kerma (i.e., *dose to air*) 1 m above a 1.25 MeV plane source at the air-ground interface with the calculations of Béck and de Planque (1968) and with the calculations and measurements given in the Shielding Benchmark Problems report (Garrett, 1968). Excellent agreement was found in both cases.

The angular dependence of the air kerma one meter above the air-ground interface is shown in Figs. II.5 through II.8 for 100 keV sources at various depths. The ninety-degree angle corresponds to radiation incident from the horizon. In these figures, one should note the relative importance of the scattered and unscattered components of the kerma and the changes in the angular distributions with increasing depth.

Organ dose from an isotropic field

The radiation fields for the submersion and water immersion sources are isotropic, neglecting the small effect on the incoming angular current caused by the presence of the phantom. The organ dose due to an isotropic field was computed using the continuous energy Monte Carlo photon transport code ALGAMP (Ryman and Eckerman, 1993), which is an updated and combined version of the original ALGAM (Warner and Craig, 1968) and BRHGAM (Warner, 1973) codes incorporating the Cristy phantom series (Cristy and Eckerman, 1987). As described in Appendix B, a modified version of the adult hermaphrodite phantom was used for this work. Organ doses in ALGAMP are estimated by scoring energy deposition in all organs except skeletal tissues. A collision-density fluence estimator for the skeleton is combined with fluence-to-dose conversion factors for active marrow and bone surface (Eckerman, 1984; Eckerman and Cristy, 1984; Kerr and Eckerman, 1985, 1987) to estimate doses for those organs.

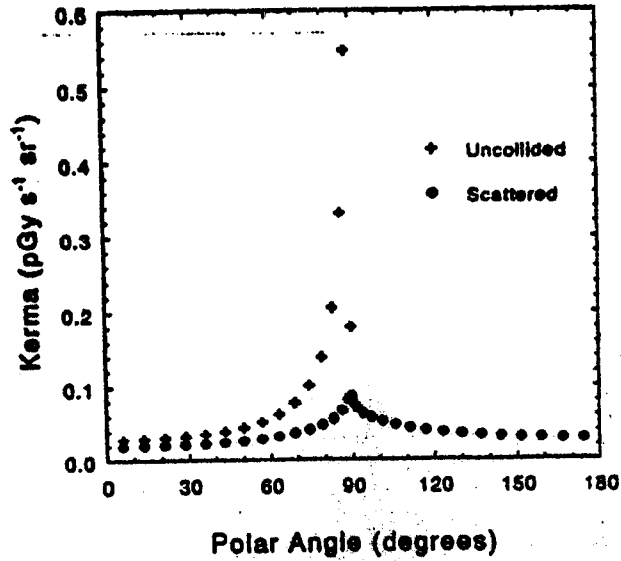


Fig. II.5. Angular dependence of air kerma for a 1 Bq m^{-3} 100 keV isotropic plane surface source.

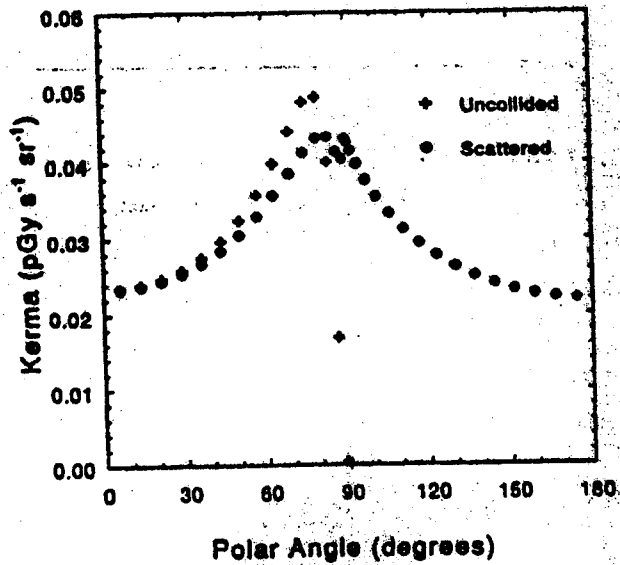


Fig. II.6. Angular dependence of air kerma for a 1 Bq m^{-3} 100 keV isotropic plane source 0.2 mean free paths deep.

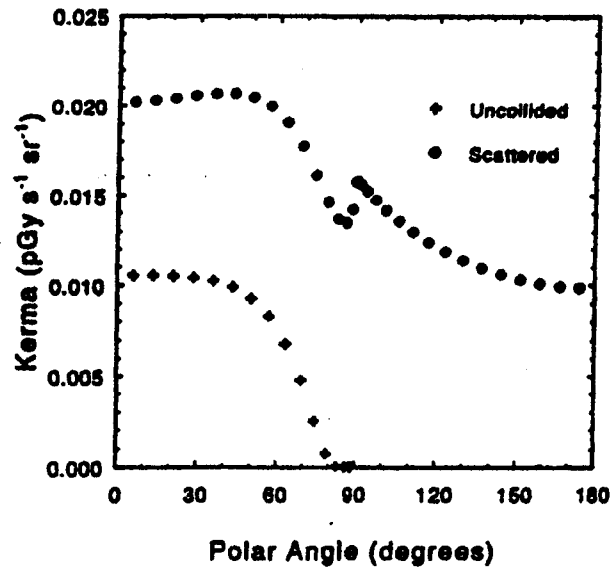


Fig. II.7. Angular dependence of air kerma for a 1 Bq m⁻³ 100 keV isotropic plane source 1 mean free path deep.

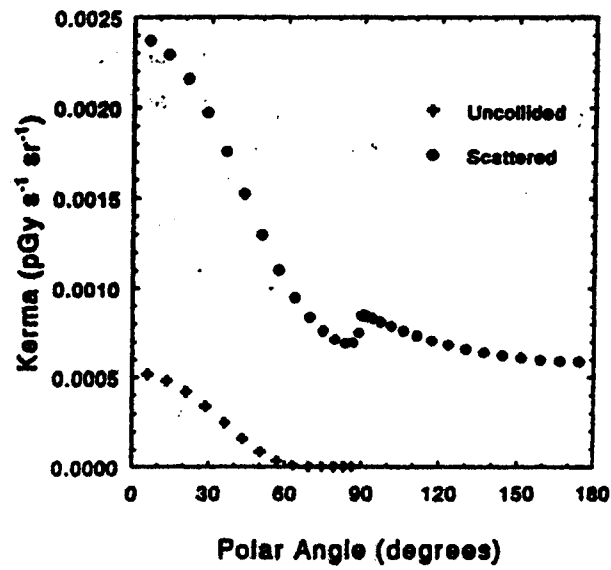


Fig. II.8. Angular dependence of air kerma for a 1 Bq m⁻³ 100 keV isotropic plane source 4 mean free paths deep.

Calculations were performed for twelve monoenergetic sources ranging from 0.01 to 5.0 MeV. These were carried out using a cosine current source, which corresponds to an isotropic fluence, sampled uniformly on the curved and end surfaces of a cylinder surrounding the phantom. Ten million histories were sampled for each calculation. The organ doses from the monoenergetic sources incident on the phantom were folded with the spectra generated by the PHOFLUX code for the air submersion and water immersion sources and normalized to unit source strength to produce the final organ dose coefficients for monoenergetic sources in contaminated air and water, presented in Tables II.4 and II.5. The coefficients include those for effective dose equivalent (h_e), effective dose (e) using the ICRP 60 weighting factors, and air kerma (k_{AIR}) or water kerma (k_{WATER}). Note that air kerma and water kerma are doses to air and water, not to tissue free in air or water. Since the dose coefficients are inversely proportional to the density of the source medium, scaling to a different density is straightforward.

Organ dose from contaminated soil

The uncollided and scattered angular fluences from an isotropic plane source of radiation were computed as a function of energy, angle, and height above the air-ground interface as described earlier. These fluence data were used to construct an angular current source on a cylinder surrounding the phantom as a function of position, energy, and polar angle. It may be noted that the angular current is given by the relationship $j(\vec{r}, E, \vec{\Omega}) = \vec{\Omega} \cdot \vec{n} \Phi(\vec{r}, E, \vec{\Omega})$ where \vec{n} is the outward-directed normal to the surface. For the top and bottom surfaces of the cylinder, the construction of the angular current source is obvious, since $\vec{\Omega} \cdot \vec{n}$ is just the absolute value of the polar angle used in the discrete ordinates calculations. On the side of the cylinder, $\vec{\Omega} \cdot \vec{n}$ is not an angle used in the calculations. Saito et al. (1990) developed two approximations for the relationship between the angular fluence and the current, but no approximation is necessary. The angular fluence is isotropic with respect to an azimuthal angle about the normal to the source plane, due to the symmetry of the one-dimensional radiation field, so the angular current, as a function of polar angle, can be computed analytically from the angular fluence data.

A calculation of organ doses was performed using ALGAMP (Ryman and Eckerman, 1993) for each of the 72 combinations of source energy and plane source depth, sampling the photon energy, angle, and position from cumulative distribution functions corresponding to the angular current sources described above. As for the calculations for isotropic sources in air and water, ten million histories were generated for each calculation. Since the discrete ordinates calculations were performed for a first-collision source generated by a unit strength plane source, the organ dose coefficients are computed directly by the Monte Carlo calculations; no

further normalization is needed. For the 10, 15, and 20 keV sources (primarily at 10 keV), a few of the organ dose coefficients were estimated to be zero, since low-energy photons are not very penetrating, and small organs (e.g., ovaries) are often missed by those few photons which do penetrate the body to that depth. For a few organs, the coefficients of variation were so large that their dose coefficients were judged to be unreliable. The dose coefficients for those organs were also set to zero. However, the procedure described below for integrating organ dose coefficients for plane sources over source depth to obtain dose coefficients for volume sources involves the logarithm of the dose coefficients; therefore, dose coefficients cannot be zero. Even had there been no numerical difficulties, the prudent approach was to assign nonzero values to all dose coefficients. Therefore, in the tabulations for monoenergetic sources, the zero values were replaced by values from a log-log extrapolation as a function of source energy. The dependence of the organ dose coefficients on energy shows this to be a conservative approach. As a practical matter, the values of the dose coefficients obtained by extrapolation are so small, compared to the dose coefficients for the other organs, that they have no observed influence on the coefficients for effective dose equivalent.

The organ dose coefficients for isotropic plane sources at the six source depths were integrated over source depth to compute organ dose coefficients for uniformly distributed volume sources having thicknesses of 1, 5, and 15 cm, and for an effectively infinite source (4 mean free paths thick). If $h_{T,P}(E,\tau)$ is the dose coefficient (Sv per Bq s m⁻²) for tissue T for a plane isotropic source at energy E and depth τ (mean free paths), then the dose coefficient $h_{T,L}(E)$ (Sv per Bq-s m⁻³) for a volumetric source extending from the air-ground interface to depth L (cm) is just

$$h_{T,L}(E) = \frac{1}{\mu} \int_0^L d\tau h_{T,P}(E,\tau) , \quad (10)$$

where μ is the linear attenuation coefficient for soil at energy E . The dose coefficients for each organ $h_{T,P}(E,\tau)$ at the six source depths were interpolated on a fine grid using a log-linear Hermite cubic spline (Fritsch and Carlson, 1980). The interpolated data were then numerically integrated. The organ dose coefficients are presented in Tables II.6 through II.11 for plane sources at the six source depths, and in Tables II.12 through II.15 for the four volumetric sources. The coefficients for the plane sources do not need to be scaled for different soil densities, since depths are in mean free paths. Coefficients for a source with finite thickness expressed in cm cannot be scaled. Coefficients for a source with finite thickness expressed in mean free paths are inversely proportional to soil density, as shown by Chen (1991), as are those for an infinitely thick source.

Table II.4. Organ Dose (Gy per Bq s m⁻³) from a Monoenergetic Semi-infinite Cloud Source

Organ/Tissue	Emitted photon energy (MeV)											
	1.0E-02	1.5E-02	2.0E-02	3.0E-02	5.0E-02	7.0E-02	1.0E-01	2.0E-01	5.0E-01	1.0E+00	2.0E+00	5.0E+00
ADRENALS	2.489E-22	7.806E-20	4.213E-18	1.086E-16	8.124E-16	1.746E-15	3.092E-15	7.205E-15	1.944E-14	4.044E-14	8.798E-14	2.491E-13
B SURFACE	1.034E-18	2.736E-17	1.810E-16	1.158E-15	5.822E-15	9.896E-15	1.432E-14	2.291E-14	4.155E-14	7.265E-14	1.385E-13	3.540E-13
BRAIN	9.062E-24	1.718E-20	3.466E-18	1.502E-16	1.138E-15	2.355E-15	4.060E-15	9.270E-15	2.475E-14	5.228E-14	1.109E-13	2.838E-13
BREASTS	5.061E-18	8.567E-17	2.325E-16	7.726E-16	2.105E-15	3.398E-15	5.188E-15	1.071E-14	2.878E-14	5.502E-14	1.141E-13	2.894E-13
ESOPHAGUS	1.054E-22	2.067E-20	8.300E-19	4.884E-17	6.130E-16	1.522E-15	2.866E-15	7.008E-15	1.906E-14	4.168E-14	8.078E-14	2.577E-13
ST WALL	4.492E-21	4.577E-19	1.188E-17	1.688E-16	1.024E-15	2.078E-15	3.531E-15	7.852E-15	2.067E-14	4.327E-14	8.491E-14	2.855E-13
SI WALL	3.178E-23	1.840E-20	1.751E-18	7.108E-17	7.021E-16	1.614E-15	2.932E-15	8.856E-15	1.834E-14	3.873E-14	8.820E-14	2.513E-13
ULI WALL	4.831E-23	3.145E-20	2.877E-18	8.884E-17	7.881E-16	1.758E-15	3.134E-15	7.214E-15	1.818E-14	4.003E-14	9.008E-14	2.548E-13
LLI WALL	4.951E-21	3.529E-20	1.522E-18	6.846E-17	7.148E-16	1.835E-15	2.860E-15	6.934E-15	1.868E-14	4.063E-14	8.867E-14	2.578E-13
G BLADDER	8.828E-22	8.684E-20	1.365E-18	8.421E-17	7.851E-16	1.731E-15	3.020E-15	7.011E-15	1.800E-14	4.027E-14	9.000E-14	2.818E-13
HEART	1.039E-21	6.051E-19	8.347E-18	1.301E-16	8.232E-16	1.887E-15	3.442E-15	7.778E-15	2.042E-14	4.318E-14	8.432E-14	2.878E-13
KIDNEYS	1.428E-20	1.128E-18	2.415E-17	2.484E-16	1.143E-15	2.193E-15	3.843E-15	7.973E-15	2.077E-14	4.382E-14	9.472E-14	2.833E-13
LIVER	2.564E-21	3.292E-19	8.806E-18	1.653E-16	1.036E-15	2.113E-15	3.810E-15	8.028E-15	2.089E-14	4.398E-14	9.592E-14	2.851E-13
LUNGS	3.499E-21	4.348E-19	1.275E-17	2.178E-16	1.266E-15	2.487E-15	4.147E-15	9.017E-15	2.324E-14	4.832E-14	1.037E-13	2.827E-13
MUSCLE	2.003E-18	2.477E-17	9.434E-17	3.827E-16	1.460E-15	2.507E-15	4.064E-15	8.801E-15	2.271E-14	4.734E-14	1.011E-13	2.727E-13
OVARIES	6.084E-23	9.552E-21	3.280E-19	4.080E-17	6.400E-16	1.483E-15	2.788E-15	6.708E-15	1.734E-14	4.155E-14	8.810E-14	2.598E-13
PANCREAS	4.182E-23	7.820E-21	3.084E-19	4.870E-17	6.430E-16	1.546E-15	2.865E-15	6.850E-15	1.821E-14	3.897E-14	8.804E-14	2.508E-13
R MARROW	1.939E-19	4.826E-18	2.844E-17	1.721E-16	9.931E-16	1.876E-15	3.538E-15	8.341E-15	2.238E-14	4.777E-14	1.038E-13	2.873E-13
SKIN	1.138E-18	3.038E-16	5.261E-16	1.835E-15	2.239E-15	3.514E-15	5.314E-15	1.101E-14	2.774E-14	5.821E-14	1.184E-13	3.030E-13
SPLEEN	2.533E-22	1.001E-19	6.887E-18	1.518E-16	1.923E-15	2.114E-15	3.803E-15	8.028E-15	2.103E-14	4.415E-14	9.590E-14	2.874E-13
TESTES	6.587E-18	2.868E-17	1.288E-16	5.408E-16	1.889E-15	2.857E-15	4.432E-15	9.354E-15	2.341E-14	4.859E-14	1.014E-13	2.818E-13
THYMUS	1.906E-20	1.368E-18	2.846E-17	3.327E-16	1.243E-15	2.388E-15	3.930E-15	8.528E-15	2.154E-14	4.518E-14	1.015E-13	2.889E-13
THYROID	4.389E-20	1.122E-17	8.478E-17	4.311E-16	1.532E-15	2.788E-15	4.374E-15	9.394E-15	2.384E-14	4.882E-14	1.052E-13	2.978E-13
U BLADDER	8.251E-21	6.043E-19	1.220E-17	1.818E-16	8.478E-16	1.847E-15	3.337E-15	7.432E-15	1.940E-14	3.973E-14	9.174E-14	2.530E-13
UTERUS	8.773E-22	5.780E-20	1.071E-18	5.788E-17	8.582E-16	1.548E-15	2.853E-15	6.730E-15	1.787E-14	3.848E-14	8.730E-14	2.484E-13
Hg	1.103E-18	2.001E-17	8.839E-17	4.229E-16	1.574E-15	2.829E-15	4.530E-15	9.561E-15	2.397E-14	4.961E-14	1.050E-13	2.858E-13
e	1.651E-18	1.438E-17	8.028E-17	3.852E-16	1.271E-15	2.395E-15	3.955E-15	8.835E-15	2.220E-14	4.651E-14	9.970E-14	2.785E-13
Am	8.748E-16	8.812E-16	1.305E-15	1.886E-15	2.785E-15	3.880E-15	8.358E-15	1.880E-14	5.897E-14	1.228E-13	2.384E-13	5.825E-13

123

Table II.5. Organ Dose (Gy per Bq m²) from a Nonmergetic Infinite Pool Source

Organ/Tissue	Emitted photon energy (MeV)											
	1.0E-02	1.5E-02	2.0E-02	3.0E-02	5.0E-02	7.0E-02	1.0E-01	2.0E-01	5.0E-01	1.0E+00	5.0E+00	
ADRENALS	5.748E-25	1.776E-22	9.682E-21	2.333E-19	1.854E-18	3.828E-18	6.871E-18	1.578E-17	4.221E-17	6.753E-17	1.803E-16	5.430E-16
B SURFACE	2.308E-21	6.397E-20	3.804E-19	2.718E-18	1.293E-17	2.878E-17	3.216E-17	5.960E-17	9.107E-17	1.562E-16	3.002E-16	7.810E-16
BRAIN	2.082E-26	4.008E-23	8.108E-21	3.497E-19	2.602E-18	5.307E-18	9.034E-18	2.031E-17	5.376E-17	1.132E-16	2.400E-16	6.403E-16
BREASTS	1.168E-20	1.536E-18	5.474E-18	1.820E-17	4.808E-17	7.784E-17	1.170E-16	2.365E-16	5.036E-16	1.194E-15	2.471E-15	6.329E-15
BROTHAOS	2.434E-25	4.627E-23	1.643E-21	1.060E-19	1.382E-18	3.408E-18	6.343E-18	1.531E-17	4.133E-17	9.016E-17	1.964E-16	5.816E-16
ST WALL	1.037E-23	1.060E-21	2.737E-20	3.698E-19	2.348E-18	4.890E-18	7.866E-18	1.722E-17	4.491E-17	9.372E-17	2.054E-16	5.768E-16
SI WALL	7.334E-28	4.527E-23	4.008E-21	1.654E-19	1.598E-18	3.422E-18	6.502E-18	1.500E-17	3.861E-17	8.398E-17	1.909E-16	5.480E-16
ULI WALL	1.116E-25	7.340E-23	6.003E-21	2.257E-19	1.822E-18	3.853E-18	6.860E-18	1.578E-17	4.159E-17	8.398E-17	1.849E-16	5.480E-16
LLI WALL	1.163E-23	6.252E-21	3.540E-20	1.613E-19	1.828E-18	3.870E-18	6.564E-18	1.517E-17	4.037E-17	8.794E-17	1.818E-16	5.329E-16
G BLADDER	2.030E-24	1.561E-22	3.188E-21	1.054E-19	1.790E-18	3.661E-18	6.708E-18	1.535E-17	4.103E-17	8.718E-17	1.967E-16	5.710E-16
HEART	2.399E-24	1.413E-21	1.830E-20	3.039E-19	2.111E-18	4.430E-18	7.653E-18	1.704E-17	4.435E-17	9.352E-17	2.041E-16	5.840E-16
KIDNEYS	3.297E-23	2.437E-21	5.663E-20	5.771E-19	2.831E-18	4.967E-18	8.138E-18	1.751E-17	4.516E-17	9.450E-17	2.050E-16	5.741E-16
LIVER	5.921E-24	7.607E-22	2.315E-20	3.461E-19	2.360E-18	4.768E-18	8.412E-18	1.761E-17	4.538E-17	9.322E-17	2.075E-16	5.760E-16
LUNGS	8.960E-24	1.015E-21	2.988E-20	5.086E-19	2.804E-18	5.821E-18	9.251E-18	1.980E-17	5.031E-17	1.051E-16	2.244E-16	6.184E-16
MUSCLE	4.624E-21	5.783E-20	2.220E-19	9.230E-18	3.237E-17	5.762E-17	9.107E-17	1.938E-17	4.941E-17	1.028E-16	2.188E-16	5.843E-16
OVARIES	1.405E-25	2.231E-23	7.030E-22	8.452E-20	1.452E-18	3.323E-18	6.130E-18	1.466E-17	3.782E-17	8.892E-17	1.927E-16	5.639E-16
PANCREAS	9.657E-26	1.848E-23	7.216E-22	1.082E-20	1.461E-18	3.463E-18	6.345E-18	1.497E-17	3.850E-17	8.434E-17	1.904E-16	5.463E-16
R HARBOW	4.478E-22	1.128E-20	6.217E-20	4.035E-19	3.140E-18	4.53E-18	7.867E-18	1.826E-17	4.860E-17	1.034E-16	2.246E-16	6.363E-16
SKIN	2.627E-19	7.113E-18	1.343E-16	2.490E-16	3.226E-16	8.048E-16	1.202E-15	2.433E-15	6.648E-15	1.230E-14	2.321E-14	6.042E-14
SPLEEN	5.648E-25	3.377E-22	1.561E-20	3.543E-19	2.341E-18	4.768E-18	8.021E-18	1.760E-17	4.570E-17	9.582E-17	2.075E-16	5.830E-16
TESTES	1.521E-21	6.233E-20	3.050E-19	1.277E-18	3.018E-18	6.522E-18	9.968E-18	2.062E-17	5.090E-17	1.054E-16	2.185E-16	6.143E-16
THYRUS	4.608E-23	3.162E-21	6.192E-20	5.018E-19	2.663E-18	5.323E-18	9.775E-18	2.187E-17	5.693E-17	1.187E-16	2.197E-16	5.842E-16
THYROID	1.013E-22	2.831E-20	1.013E-18	3.543E-18	6.158E-18	9.808E-18	2.067E-17	5.187E-17	1.062E-16	2.270E-16	5.453E-16	1.502E-15
U BLADDER	1.905E-23	1.412E-21	2.601E-20	3.778E-19	4.322E-18	7.432E-18	1.630E-17	4.215E-17	8.604E-17	1.843E-16	4.182E-16	1.140E-15
UTERUS	2.026E-24	1.356E-22	2.508E-21	1.322E-19	1.462E-18	3.471E-18	6.321E-18	1.471E-17	3.078E-17	6.331E-17	1.408E-16	3.437E-16
b ₁	2.546E-21	4.878E-20	2.165E-19	9.412E-18	3.638E-18	6.432E-18	1.013E-17	2.103E-17	5.310E-17	1.073E-16	2.373E-16	6.232E-16
b ₂	3.812E-21	3.958E-20	1.418E-19	7.178E-18	2.638E-18	4.598E-18	6.641E-18	1.097E-17	4.628E-17	1.068E-16	2.158E-16	6.028E-16
b ₃ WATER	1.615E-16	2.463E-16	3.164E-16	6.576E-16	6.508E-16	9.384E-16	1.373E-15	4.681E-15	1.664E-14	2.878E-14	5.738E-14	1.368E-13

Table II.6. Organ Dose (Gy per Bq s m⁻²) from a Monoenergetic Plane Source at the Air-ground Interface

Organ/Tissue	Emitted photon energy (MeV)											
	1.0E-02	1.5E-02	2.0E-02	3.0E-02	5.0E-02	7.0E-02	1.0E-01	2.0E-01	5.0E-01	1.0E+00	2.0E+00	5.0E+00
ADRENALS	1.138E-20	1.378E-19	8.100E-19	8.829E-18	3.003E-17	4.905E-17	7.476E-17	1.834E-16	4.167E-16	8.407E-16	1.489E-15	3.418E-15
B SURFACE	1.888E-19	5.795E-18	2.454E-17	8.315E-17	2.074E-16	2.529E-16	2.826E-16	3.747E-16	7.253E-16	1.292E-15	2.270E-15	4.727E-15
BRAIN	9.716E-25	1.422E-21	2.505E-19	7.655E-18	3.318E-17	5.175E-17	7.818E-17	1.689E-16	4.442E-16	8.771E-16	1.827E-15	3.457E-15
BREASTS	1.066E-18	1.314E-17	3.022E-17	4.889E-17	5.724E-17	6.900E-17	9.393E-17	1.950E-16	4.989E-16	9.570E-16	1.747E-15	3.708E-15
ESOPHAGUS	4.655E-24	6.456E-22	2.137E-20	2.864E-18	2.335E-17	4.246E-17	6.882E-17	1.501E-16	4.016E-16	8.020E-16	1.506E-15	3.335E-15
ST WALL	1.567E-21	1.045E-19	2.057E-18	1.409E-17	3.827E-17	5.722E-17	8.321E-17	1.739E-16	4.433E-16	8.868E-16	1.645E-15	3.583E-15
SI WALL	1.029E-23	4.575E-21	3.460E-19	6.746E-18	3.023E-17	5.044E-17	7.647E-17	1.638E-16	4.321E-16	8.735E-16	1.663E-15	3.562E-15
ULI WALL	9.988E-24	5.829E-21	5.348E-19	8.882E-18	3.318E-17	5.334E-17	8.010E-17	1.887E-16	4.413E-16	8.786E-16	1.674E-15	3.588E-15
LLI WALL	7.303E-22	2.781E-20	3.701E-19	6.890E-18	3.184E-17	5.225E-17	7.958E-17	1.690E-16	4.479E-16	8.100E-16	1.700E-15	3.590E-15
G BLADDER	2.445E-21	4.738E-20	3.893E-19	7.527E-18	3.095E-17	4.853E-17	6.117E-17	1.383E-16	4.241E-16	8.253E-16	1.593E-15	3.335E-15
HEART	3.275E-21	1.132E-19	1.398E-18	1.088E-17	3.581E-17	5.463E-17	8.135E-17	1.673E-16	4.392E-16	8.748E-16	1.628E-15	3.478E-15
KIDNEYS	7.164E-21	3.061E-19	4.384E-18	2.080E-17	4.186E-17	5.788E-17	8.382E-17	1.728E-16	4.474E-16	8.866E-16	1.686E-15	3.562E-15
LIVER	9.768E-22	7.800E-20	1.745E-18	1.393E-17	3.926E-17	5.808E-17	8.388E-17	1.734E-16	4.457E-16	8.864E-16	1.684E-15	3.519E-15
LUNGS	1.387E-21	9.981E-20	2.074E-18	1.710E-17	4.455E-17	6.287E-17	8.966E-17	1.828E-16	4.732E-16	9.207E-16	1.725E-15	3.636E-15
MUSCLE	9.151E-19	7.986E-18	1.752E-17	3.289E-17	4.986E-17	6.588E-17	9.326E-17	1.962E-16	5.112E-16	9.988E-16	1.831E-15	3.780E-15
OVARIES	1.333E-19	5.101E-19	1.322E-18	5.058E-18	2.743E-17	5.160E-17	7.486E-17	1.656E-16	4.734E-16	8.337E-16	1.578E-15	3.673E-15
PANCREAS	4.673E-23	3.262E-21	6.833E-20	4.830E-18	2.781E-17	4.843E-17	7.402E-17	1.582E-16	4.087E-16	8.215E-16	1.595E-15	3.539E-15
R MARRON	3.072E-20	9.539E-19	3.647E-18	1.243E-17	3.312E-17	5.353E-17	8.327E-17	1.816E-16	4.778E-16	9.484E-16	1.777E-15	3.785E-15
SKIN	5.046E-17	8.798E-17	8.729E-17	7.545E-17	6.831E-17	7.882E-17	1.077E-16	2.278E-16	3.897E-16	1.133E-15	2.025E-15	4.090E-15
SPLEEN	6.389E-23	1.916E-20	1.096E-18	1.338E-17	3.978E-17	5.844E-17	8.493E-17	1.752E-16	4.462E-16	8.942E-16	1.641E-15	3.656E-15
TESTES	3.597E-19	8.241E-18	2.588E-17	4.481E-17	5.872E-17	6.817E-17	8.669E-17	1.986E-16	5.197E-16	1.004E-15	1.830E-15	3.985E-15
THYMUS	6.092E-21	2.602E-19	3.734E-18	1.885E-17	4.158E-17	6.113E-17	8.185E-17	1.859E-16	4.556E-16	8.417E-16	1.673E-15	3.513E-15
THYROID	7.423E-20	1.185E-18	8.480E-18	2.790E-17	4.863E-17	6.226E-17	9.072E-17	1.829E-16	4.844E-16	9.444E-16	1.597E-15	3.811E-15
U BLADDER	2.426E-21	1.380E-19	2.387E-18	1.479E-17	3.808E-17	5.872E-17	8.493E-17	1.715E-16	4.550E-16	8.783E-16	1.805E-15	4.038E-15
UTERUS	4.928E-22	1.578E-20	1.848E-18	5.823E-18	2.825E-17	4.874E-17	7.785E-17	1.649E-16	4.322E-16	8.633E-16	1.627E-15	3.705E-15
h _e	3.181E-19	5.147E-18	1.443E-17	3.179E-17	5.244E-17	6.815E-17	9.805E-17	1.931E-16	4.845E-16	9.610E-16	1.778E-15	3.814E-15
o	8.811E-19	4.017E-18	1.018E-17	2.367E-17	4.460E-17	6.162E-17	8.828E-17	1.841E-16	4.781E-16	9.376E-16	1.737E-15	3.731E-15
h _{AM}	1.820E-16	2.323E-16	1.881E-16	1.256E-16	8.337E-17	6.515E-17	1.117E-16	2.415E-16	6.394E-16	1.211E-15	2.122E-15	4.194E-15

25

Table II.7. Organ Dose (Gy per Bq s m⁻³) from a Monoenergetic Plane Source 0.04 Mean Free Paths Deep

Organ/Tissue	Emitted photon energy (MeV)											
	1.0E-02	1.5E-02	2.0E-02	3.0E-02	5.0E-02	7.0E-02	1.0E-01	2.0E-01	5.0E-01	1.0E+00	2.0E+00	5.0E+00
ADRENALS	0.084E-21	0.691E-20	5.847E-19	7.154E-18	2.352E-17	3.824E-17	5.934E-17	1.239E-16	3.085E-16	5.809E-16	9.712E-16	1.720E-15
B SURFACE	1.895E-19	4.681E-18	1.818E-17	6.738E-17	1.504E-16	1.800E-16	2.185E-16	2.878E-16	5.029E-16	8.174E-16	1.318E-15	2.461E-15
BRAIN	5.330E-25	0.847E-22	2.002E-18	8.001E-18	2.568E-17	4.182E-17	6.326E-17	1.346E-16	3.313E-16	6.097E-16	1.052E-15	1.949E-15
BREASTS	9.766E-19	1.112E-17	2.518E-17	3.864E-17	4.514E-17	5.584E-17	7.637E-17	1.538E-16	3.668E-16	6.446E-16	1.081E-15	1.887E-15
ESOPHAGUS	3.714E-23	2.188E-21	3.877E-20	2.354E-18	1.737E-17	3.384E-17	5.403E-17	1.125E-16	2.822E-16	5.138E-16	9.144E-16	1.802E-15
ST WALL	1.607E-21	9.244E-20	1.839E-18	1.077E-17	2.905E-17	4.427E-17	6.485E-17	1.292E-16	3.076E-16	5.671E-16	9.562E-16	1.843E-15
SI WALL	6.004E-24	3.038E-21	2.519E-19	4.857E-18	2.218E-17	3.771E-17	5.858E-17	1.208E-16	2.835E-16	5.459E-16	9.467E-16	1.815E-15
ULI WALL	3.032E-23	8.078E-21	4.249E-18	8.514E-18	2.446E-17	4.035E-17	6.128E-17	1.252E-16	3.014E-16	5.530E-16	9.377E-16	1.827E-15
LLI WALL	4.715E-21	2.783E-20	2.870E-19	5.215E-18	2.284E-17	3.804E-17	6.007E-17	1.233E-16	2.878E-16	5.540E-16	8.805E-16	1.871E-15
G BLADDER	8.335E-22	2.338E-20	2.288E-18	5.760E-18	2.312E-17	3.735E-17	5.780E-17	1.227E-16	2.835E-16	5.843E-16	8.875E-16	1.774E-15
HEART	3.335E-21	8.938E-20	1.105E-18	8.388E-18	2.878E-17	4.221E-17	6.337E-17	1.288E-16	3.144E-16	5.841E-16	9.948E-16	1.957E-15
KIDNEYS	5.090E-21	2.326E-19	3.502E-18	1.535E-17	3.124E-17	4.503E-17	6.504E-17	1.321E-16	3.154E-16	5.808E-16	9.705E-16	1.888E-15
LIVER	9.393E-22	6.670E-20	1.373E-18	1.041E-17	2.961E-17	4.490E-17	6.560E-17	1.324E-16	3.140E-16	5.879E-16	9.804E-16	1.872E-15
LUNGS	1.315E-21	8.644E-20	1.884E-18	1.302E-17	3.418E-17	4.869E-17	7.140E-17	1.418E-16	3.384E-16	6.136E-16	1.040E-15	1.983E-15
MUSCLE	7.781E-19	8.263E-18	1.338E-17	2.372E-17	3.644E-17	4.820E-17	7.034E-17	1.433E-16	3.411E-16	6.133E-16	1.035E-15	1.838E-15
OVARIES	8.755E-20	3.459E-18	8.167E-18	3.821E-18	2.044E-17	3.738E-17	5.553E-17	1.156E-16	2.857E-16	5.662E-16	9.786E-16	1.928E-15
PANCREAS	7.331E-23	3.859E-21	6.423E-20	3.381E-18	2.033E-17	3.880E-17	5.728E-17	1.181E-16	2.851E-16	5.338E-16	9.196E-16	1.789E-15
R MARROW	2.765E-20	7.848E-19	2.888E-18	8.532E-18	2.518E-17	4.134E-17	6.486E-17	1.387E-16	3.358E-16	6.138E-16	1.058E-15	2.017E-15
SKIN	4.385E-17	7.001E-17	6.782E-17	5.521E-17	5.820E-17	5.847E-17	8.131E-17	1.684E-16	3.840E-16	6.848E-16	1.148E-15	2.091E-15
SPLEEN	8.197E-23	1.854E-20	8.488E-19	8.888E-18	2.834E-17	4.548E-17	6.818E-17	1.348E-16	3.174E-16	5.573E-16	9.617E-16	1.881E-15
TESTES	3.982E-19	7.400E-18	2.042E-17	3.415E-17	4.247E-17	5.285E-17	7.341E-17	1.451E-16	3.482E-16	6.098E-16	1.062E-15	2.013E-15
THYRUS	3.028E-21	1.722E-19	3.028E-18	1.493E-17	3.287E-17	4.612E-17	6.793E-17	1.295E-16	3.281E-16	5.734E-16	9.865E-16	1.850E-15
THYROID	4.891E-20	8.844E-19	8.798E-18	1.835E-17	3.381E-17	4.783E-17	7.011E-17	1.403E-16	3.614E-16	6.508E-16	1.047E-15	2.055E-15
U BLADDER	2.128E-21	1.172E-19	2.818E-18	1.067E-17	2.863E-17	4.308E-17	6.278E-17	1.301E-16	2.973E-16	5.456E-16	8.274E-16	1.788E-15
UTERUS	2.877E-22	8.508E-21	1.187E-19	4.251E-18	2.118E-17	3.738E-17	5.864E-17	1.202E-16	2.881E-16	5.428E-16	8.122E-16	1.865E-15
h _g	3.041E-19	4.204E-18	1.164E-17	2.418E-17	3.867E-17	5.348E-17	7.342E-17	1.465E-16	3.481E-16	6.182E-16	1.053E-15	1.880E-15
σ	8.188E-19	3.248E-18	8.127E-18	1.787E-17	3.343E-17	4.778E-17	6.834E-17	1.381E-16	3.368E-16	5.836E-16	1.018E-15	1.845E-15
h _{AM}	1.687E-16	1.845E-16	1.553E-16	8.742E-17	8.543E-17	8.827E-17	8.871E-17	1.863E-16	4.588E-16	7.847E-16	1.255E-15	2.217E-15
M _{50E} (cm ⁻¹)	3.201E+01	8.853E+00	4.368E+00	1.448E+00	5.884E-01	3.484E-01	2.883E-01	2.021E-01	1.418E-01	1.035E-01	7.281E-02	4.834E-02

Table II.8. Organ Dose (Gy per Bq s m⁻³) from a Monoenergetic Plane Source 0.2 Mean Free Paths Deep

Organ/Tissue	Emitted photon energy (MeV)											
	1.0E-02	1.5E-02	2.0E-02	3.0E-02	5.0E-02	7.0E-02	1.0E-01	2.0E-01	5.0E-01	1.0E+00	2.0E+00	5.0E+00
ADRENALS	4.126E-21	5.197E-20	3.136E-19	3.850E-18	1.259E-17	2.183E-17	3.726E-17	7.526E-17	1.737E-16	2.890E-16	5.299E-16	8.074E-16
B SURFACE	1.213E-19	2.863E-18	1.067E-17	3.546E-17	8.562E-17	1.181E-16	1.469E-16	1.988E-16	3.190E-16	4.805E-16	7.264E-16	1.274E-15
BRAIN	9.963E-26	3.483E-22	1.198E-19	3.189E-18	1.512E-17	2.634E-17	4.193E-17	8.835E-17	2.017E-16	3.470E-16	5.709E-16	1.034E-15
BREASTS	7.457E-19	7.447E-18	1.526E-17	2.230E-17	2.766E-17	3.812E-17	5.173E-17	1.030E-16	2.247E-16	3.781E-16	5.988E-16	1.048E-15
ESOPHAGUS	8.055E-24	6.478E-22	1.457E-20	1.172E-18	8.428E-18	1.866E-17	3.398E-17	7.296E-17	1.747E-16	2.923E-16	5.063E-16	8.889E-16
ST WALL	1.093E-21	5.458E-20	8.752E-18	5.545E-18	1.634E-17	2.889E-17	4.161E-17	8.283E-17	1.817E-16	3.209E-16	5.186E-16	9.798E-16
SI WALL	3.537E-24	1.615E-21	1.245E-19	2.384E-18	1.203E-17	2.221E-17	3.851E-17	7.560E-17	1.707E-16	2.996E-16	4.990E-16	9.265E-16
ULI WALL	8.502E-24	3.188E-21	2.137E-19	3.237E-18	1.334E-17	2.307E-17	3.795E-17	7.804E-17	1.760E-16	3.068E-16	5.060E-16	9.239E-16
LLI WALL	2.513E-21	1.933E-20	1.832E-19	2.544E-18	1.250E-17	2.302E-17	3.739E-17	7.775E-17	1.769E-16	3.050E-16	5.102E-16	9.591E-16
G BLADDER	8.813E-22	1.537E-20	1.403E-19	3.186E-18	1.303E-17	2.313E-17	3.717E-17	7.668E-17	1.694E-16	2.994E-16	4.721E-16	1.048E-15
HEART	2.161E-21	5.742E-20	5.884E-19	4.225E-18	1.515E-17	2.560E-17	4.017E-17	8.237E-17	1.811E-16	3.165E-16	5.091E-16	9.482E-16
KIDNEYS	2.863E-21	1.266E-19	1.862E-18	8.083E-18	1.784E-17	2.702E-17	4.160E-17	8.472E-17	1.886E-16	3.155E-16	5.373E-16	9.757E-16
LIVER	5.073E-22	3.548E-20	7.225E-19	5.424E-18	1.665E-17	2.718E-17	4.205E-17	8.446E-17	1.866E-16	3.179E-16	5.244E-16	9.497E-16
LUNGS	8.680E-22	4.958E-20	8.738E-19	6.806E-18	1.881E-17	3.064E-17	4.821E-17	9.168E-17	2.036E-16	3.457E-16	5.611E-16	1.015E-15
MUSCLE	4.901E-19	3.390E-18	7.187E-18	1.246E-17	2.085E-17	3.029E-17	4.534E-17	9.183E-17	2.043E-16	3.465E-16	5.586E-16	9.939E-16
OVARIES	1.866E-20	8.848E-20	2.759E-19	1.415E-18	1.110E-17	2.143E-17	3.522E-17	7.568E-17	1.631E-16	3.062E-16	5.173E-16	8.738E-16
PANCREAS	3.617E-23	1.930E-21	3.245E-20	1.732E-18	1.114E-17	2.167E-17	3.626E-17	7.482E-17	1.689E-16	2.840E-16	4.893E-16	8.836E-16
R MARROW	2.001E-20	4.861E-19	1.768E-18	5.122E-18	1.438E-17	2.511E-17	4.144E-17	8.856E-17	2.000E-16	3.451E-16	5.685E-16	1.025E-15
SKIN	2.927E-17	4.244E-17	3.850E-17	3.034E-17	2.891E-17	3.779E-17	5.404E-17	1.092E-16	2.403E-16	4.017E-16	6.312E-16	1.092E-15
SPLEEN	7.964E-23	1.291E-20	4.773E-19	5.115E-18	1.886E-17	2.724E-17	4.171E-17	8.518E-17	1.885E-16	3.260E-16	5.329E-16	9.699E-16
TESTES	2.727E-19	4.750E-18	1.216E-17	1.874E-17	2.513E-17	3.401E-17	5.008E-17	9.933E-17	2.187E-16	3.874E-16	5.820E-16	1.102E-15
THYMUS	2.835E-21	1.136E-19	1.841E-18	7.683E-18	1.820E-17	2.968E-17	4.327E-17	8.618E-17	1.844E-16	3.364E-16	5.471E-16	1.035E-15
THYROID	4.454E-20	5.475E-19	3.247E-18	8.721E-18	1.851E-17	2.848E-17	4.290E-17	8.572E-17	1.879E-16	3.098E-16	5.206E-16	1.043E-15
U BLADDER	1.984E-21	7.429E-20	8.675E-19	5.455E-18	1.531E-17	2.545E-17	3.872E-17	8.110E-17	1.787E-16	3.143E-16	5.291E-16	9.500E-16
UTERUS	1.983E-22	6.008E-21	6.806E-20	2.083E-18	1.140E-17	2.174E-17	3.601E-17	7.371E-17	1.897E-16	3.030E-16	4.812E-16	8.133E-16
Hg	2.176E-19	2.710E-18	8.816E-18	1.317E-17	2.308E-17	3.352E-17	4.935E-17	9.662E-17	2.107E-16	3.555E-16	5.729E-16	1.052E-15
o	4.132E-19	2.045E-18	4.701E-18	8.582E-18	1.818E-17	2.942E-17	4.478E-17	8.976E-17	1.988E-16	3.381E-16	5.506E-16	1.016E-15
K _{AB}	1.244E-16	1.255E-16	8.185E-17	5.939E-17	4.048E-17	4.523E-17	6.137E-17	1.248E-16	2.800E-16	4.809E-16	7.029E-16	1.173E-15
M _{50E} (cm ⁻¹)	3.201E+01	8.653E+00	4.308E+00	1.448E+00	5.084E-01	3.404E-01	2.865E-01	2.021E-01	1.418E-01	1.035E-01	7.261E-02	4.834E-02

Table II.8. Organ Dose (Gy per Bq s m⁻³) from a Monoenergetic Flame Source 1.0 Mm Free Paths Deep

Organ/Tissue	Emitted photon energy (MeV)											
	1.0E-02	1.5E-02	2.0E-02	3.0E-02	5.0E-02	7.0E-02	1.0E-01	2.0E-01	5.0E-01	1.0E+00	2.0E+00	5.0E+00
ADRENALS	4.639E-22	6.413E-21	4.134E-20	3.715E-19	2.984E-18	6.518E-18	1.175E-17	2.782E-17	5.501E-17	8.043E-17	1.248E-16	2.078E-16
B SURFACE	2.808E-20	5.271E-19	1.845E-18	6.504E-18	2.038E-17	3.512E-17	5.308E-17	8.323E-17	1.105E-16	1.538E-16	2.023E-16	3.052E-16
BRAIN	3.732E-26	7.488E-23	1.850E-20	5.517E-19	3.542E-18	7.571E-18	1.412E-17	3.188E-17	6.496E-17	8.844E-17	1.467E-16	2.321E-16
BREASTS	2.168E-19	1.694E-18	3.215E-18	4.831E-18	7.347E-18	1.143E-17	1.868E-17	3.072E-17	7.845E-17	1.134E-16	1.613E-16	2.500E-16
ESOPHAGUS	9.305E-25	0.385E-23	2.044E-21	1.842E-19	2.147E-18	5.387E-18	1.097E-17	2.585E-17	5.178E-17	8.325E-17	1.225E-16	1.964E-16
ST WALL	1.044E-22	6.787E-21	1.312E-19	8.811E-19	3.886E-18	7.563E-18	1.365E-17	2.882E-17	5.824E-17	8.865E-17	1.303E-16	2.183E-16
SI WALL	2.815E-25	1.778E-22	1.727E-20	3.787E-19	2.818E-18	6.003E-18	1.170E-17	2.674E-17	5.376E-17	8.387E-17	1.255E-16	2.086E-16
ULI WALL	2.411E-25	2.268E-22	2.915E-20	3.082E-19	2.968E-18	6.440E-18	1.218E-17	2.747E-17	5.515E-17	8.569E-17	1.275E-16	2.107E-16
LLI WALL	3.881E-22	3.532E-21	2.453E-20	4.228E-19	2.784E-18	6.324E-18	1.209E-17	2.777E-17	5.840E-17	8.654E-17	1.275E-16	2.120E-16
G BLADDER	9.214E-23	2.103E-21	1.834E-20	4.413E-19	2.844E-18	6.418E-18	1.128E-17	2.877E-17	5.282E-17	9.240E-17	1.320E-16	2.188E-16
HEART	4.875E-14	1.044E-12	9.181E-12	7.074E-11	3.415E-10	7.178E-10	1.329E-09	2.832E-09	5.784E-09	8.808E-09	1.298E-08	2.090E-08
KIDNEYS	4.288E-22	1.892E-20	2.778E-19	1.410E-18	4.171E-18	7.817E-18	1.405E-17	3.076E-17	6.224E-17	9.147E-17	1.351E-16	2.142E-16
LIVER	6.270E-23	4.821E-21	1.050E-19	8.300E-19	3.801E-18	7.888E-18	1.385E-17	3.057E-17	6.053E-17	9.184E-17	1.338E-16	2.176E-16
LUNGS	1.054E-22	6.875E-21	1.332E-19	1.167E-18	4.538E-18	8.745E-18	1.582E-17	3.353E-17	6.822E-17	1.000E-16	1.446E-16	2.281E-16
MUSCLE	6.829E-20	6.457E-19	1.268E-18	2.370E-18	5.087E-18	8.927E-18	1.532E-17	3.462E-17	6.788E-17	1.027E-16	1.488E-16	2.334E-16
OVARIES	1.528E-21	9.705E-21	3.883E-20	2.288E-19	2.351E-18	5.850E-18	1.131E-17	2.728E-17	5.308E-17	8.095E-17	1.174E-16	1.731E-16
PANCREAS	2.357E-24	1.708E-22	3.567E-21	2.585E-19	2.418E-18	5.768E-18	1.141E-17	2.836E-17	5.268E-17	8.152E-17	1.240E-16	2.084E-16
R MAMMARY	4.523E-21	8.205E-20	3.004E-19	8.501E-18	3.353E-18	7.128E-18	1.368E-17	3.188E-17	6.528E-17	9.974E-17	1.468E-16	2.382E-16
SKIN	6.885E-18	8.823E-18	7.717E-18	6.377E-18	7.825E-18	1.188E-17	1.842E-17	4.174E-17	8.288E-17	1.228E-16	1.728E-16	2.848E-16
SPLEEN	1.119E-24	8.945E-22	6.855E-20	8.524E-19	3.758E-18	7.783E-18	1.385E-17	3.071E-17	6.068E-17	8.151E-17	1.367E-16	2.218E-16
TESTES	7.712E-20	1.102E-18	2.603E-18	4.088E-18	6.548E-18	1.087E-17	1.767E-17	3.799E-17	7.649E-17	1.121E-16	1.671E-16	2.254E-16
THYMUS	2.626E-22	1.470E-20	2.556E-19	1.398E-18	4.618E-18	8.538E-18	1.473E-17	3.258E-17	6.287E-17	8.807E-17	1.282E-16	2.282E-16
THYROID	2.522E-21	4.544E-20	3.355E-19	1.432E-18	4.487E-18	8.053E-18	1.442E-17	3.107E-17	6.038E-17	8.222E-17	1.418E-16	1.918E-16
U BLADDER	3.012E-22	1.082E-20	1.385E-19	8.184E-19	3.598E-18	7.122E-18	1.338E-17	2.882E-17	5.822E-17	8.284E-17	1.278E-16	2.188E-16
UTERUS	3.038E-23	8.138E-22	1.821E-20	3.688E-19	2.474E-18	5.748E-18	1.123E-17	2.833E-17	5.388E-17	8.168E-17	1.278E-16	2.438E-16
hg	5.813E-20	8.007E-19	1.375E-18	2.863E-18	5.705E-18	1.002E-17	1.710E-17	3.635E-17	7.118E-17	1.055E-16	1.533E-16	2.331E-16
o	1.005E-19	4.440E-19	8.353E-19	1.894E-18	4.821E-18	8.507E-18	1.528E-17	3.318E-17	6.588E-17	8.894E-17	1.448E-16	2.241E-16
KAR	3.447E-17	2.838E-17	1.840E-17	1.217E-17	1.117E-17	1.590E-17	2.315E-17	4.831E-17	8.888E-17	1.472E-16	2.810E-16	2.837E-16
μ_{SOIL} (cm ⁻¹)	3.201E+01	8.853E+00	4.388E+00	1.448E+00	5.884E-01	3.484E-01	2.883E-01	2.821E-01	1.410E-01	1.835E-01	7.281E-02	4.634E-02

28